RESEARCH ARTICLE

INTERNATIONAL MICROBIOLOGY (2009) 12:49-57
DOI: 10.2436/20.1501.01.81 ISSN: 1139-6709 **www.im.microbios.org**

INTERNATIONAL MICROBIOLOGY

Effect of oxidative stress on the growth of magnetic particles in *Magnetospirillum magneticum*

Radu Popa,[1*] Wen Fang,[1] Kenneth H. Nealson,[2] Virginia Souza-Egipsy,[3] Thelma S. Berquó,[4] Subir K. Banerjee,[4] Lee R. Penn[4]

[1]Portland State University, Portland, Oregon, USA. [2]University of Southern California, Los Angeles, California, USA. [3]Center for Astrobiology, Torrejón de Ardoz, Madrid, Spain. [4]University of Minnesota, Minneapolis, Minnesota, USA

Received 7 February 2009 · Accepted 15 March 2009

Summary. Individual magnetosome-containing magnetic mineral particles (MMP) from magnetotactic bacteria grow rapidly such that only a small fraction (<5%) of all magnetosomes contain dwarf (≤20 nm) MMP. Studies of the developmental stages in the growth of MMP are difficult due to the absence of techniques to separate dwarf from mature particles and because the former are sensitive to extraction procedures. Here, O_2 stress was used to inhibit MMP expression in *Magnetospirillum magneticum* strain AMB-1. In addition, defined growth conditions not requiring chemical monitoring or manipulation of the gas composition during growth resulted in the production of cells containing high numbers of dwarf MMP. Cells exposed to different incubation treatments and cells with dwarf MMP were compared to cells with normal MMP with respect to growth, respiration, iron content, and relative magnetite load (RML). The cells were examined by electron microscopy, low temperature magnetometry, X-ray diffraction (XRD), and Mössbauer spectroscopy. In the 0–110 μM O_2(aq) range, growth was positively correlated with [O_2] and negatively correlated with RML. Most MMP formed during exponential growth of the cells. At 50–100 μM O_2(aq) with stirring (150 rpm) and <30% O_2 loss during incubation, MMP expression was strongly inhibited whereas MMP nucleation was not. Cells highly enriched (~95%) in dwarf MMP were obtained at the end of the exponential phase in stirred (150 rpm) cultures containing 45 μM O_2(aq). Only one dwarf MMP formed in each MMP vesicle and the chain arrangement was largely preserved. O_2-stress-induced dwarf MMP consisted of non-euhedral spheroids (~25 nm) that were similar in shape and size to immature MMP from normal cells. They consisted solely of magnetite, with a single domain signature, no superparamagnetic behavior, and magnetic signatures, Fe(II)/Fe(III) ratios, and XRD patterns very similar to those of mature MMP. These results show that O_2 stress in liquid cultures amended with an inorganic redox buffer ($S_2O_3^{2-}/S^0$) can be used to produce abundant dwarf MMP that are good proxies for studying MMP development. [**Int Microbiol** 2009; 12(1):49-57]

Key words: *Magnetospirillum magneticum* AMB-1 · magnetotactic bacteria · magnetosomes · biomineralization · magnetite · dwarf MMP

Introduction

Magnetosomes are membrane-bound organelles containing magnetic mineral particles (MMP). They are present in magnetotactic bacteria (MB) [1,2,6,7,13,19,42] as well as in many eukaryotes [20,46]. When aligned in chains, magnetosomes increase the magnetic momentum of MB and (coupled with chemotaxis) help cells move more efficiently toward interfaces of redox comfort [4,10,43]. MMP are euhedral single-domain crystals with species- and even strain-specific shapes ranging from cuboidal, parallelepipedal, or elongated pseudoprismatic to anisotropic [3,44]. Most MB have MMP that are made of magnetite. The majority of these species belong to the α-subdivision of Proteobacteria (e.g., *Magnetospirillum*, *Magnetococcus*, magnetotactic vibrios),

***Corresponding author:** R. Popa
Biology Department
Portland State University
1719 SW 10th Ave.
Portland, OR 97201, USA
Tel. +1-5037259503. Fax +1-5037253888
E-mail: rpopa@pdx.edu

but *Desulfovibrio magneticus* belongs to the δ-subdivision of Proteobacteria [18,31], and *Magnetobacterium bavaricum* to the family Nitrospiraceae [41,42]. Most of our knowledge on the formation of MMP is derived from cultures of *Magnetospirillum* [16,21,23,29,32,34]. The biomineralization of MMP in MB includes several steps that are probably common to most species, including iron-uptake [23,28, 30,33,37], Fe(III)-reduction during or after uptake [11,33,37, 39], formation of lipid membrane-based MMP vesicles [3,21,23], accumulation of Fe(II) in the MMP vesicles coupled with an increase in the intra-vesicular pH [23,24,36], oxidation of a portion of the intravesicular Fe(II) [11,37], initiation of the MMP [11,37], growth of immature MMP to full size [8,23,35], and the organization of magnetosomes in chains [21,23,34]. Nonetheless, important questions about the formation of MMP remain unanswered.

We are interested in factors that control the growth of immature MMP to full-size MMP. In general, immature MMP are difficult to study because of their low abundance (<5% of the total MMP population) and the fact that they cannot be distinguished by optical microscopy, are sensitive to extraction procedures (dissolution and oxidation), and participate in magnetic aggregation during centrifugation and thus cannot be quantitatively separated from the overall MMP population. Our approach to the study of MMP is to produce MB cells containing a high abundance of immature (i.e., dwarf) particles.

MMP development is largely controlled by biochemical and molecular mechanisms, but environmental factors can also impair development and thus must be monitored in studies of MMP [16,17,23,36]. However, daily verification of the O_2 levels and re-adjustment of the gas composition are often impractical. In the present study, the effects of various levels of initial O_2 and liquid:gas ratios were monitored in cultures of *M. magneticum* strain AMB-1. In addition, these cultures were characterized and compared based on differences in cellular growth, respiration, magnetite abundance, and iron content. The cells were examined by transmission electron microscopy, low temperature magnetometry, Mössbauer spectroscopy, and X-ray diffractometry (XRD).

Materials and methods

Growth in microaerophilic conditions. *Magnetospirillum magneticum* strain AMB-1 ATCC 700264 [25] was grown in microaerophilic conditions with O_2 concentrations between 17 and 240 μM O_2(aq) and 1.4 mM NO_3^- as electron acceptors. The culture medium contained: 5 ml Wolfe minerals/l, 5 mM KH_2PO_4, 1.4 mM $NaNO_3$, 850 μM acetate, 200 mM ascorbate, 1.4 mM succinate, 2.47 mM tartrate, 315 μM sulfur as a $S_2O_3^{2-}$:S^0 mixture (at a ratio of 9:1, used as a reducing agent), 5 ml Wolfe vitamins mix/l, 1.25 mg lipoic acid/l, and 10 ml ferric quinate solution (16.7 mM Fe^{3+}; 10.4 mM quinic acid)/l. All reagents were purchased from Sigma. Colloidal sulfur (S^0) was obtained by acid disproportionation of $Na_2S_2O_3$. The pH of the medium was adjusted to 7. The medium was distributed in serum bottles and Hungate tubes, which were sealed with 1-cm-thick rubber stoppers and crimped, and the gas phase replaced with different O_2:N_2 gas mixtures. The Wolfe vitamins mix, lipoic acid, and iron quinate were autoclaved, filter-sterilized, and then added to the medium. O_2 and N_2 concentrations in the gas phase [O_2(g) and N_2(g)] were monitored by gas chromatography (SRI 310C instrument with a molecular sieve column and TCD detector), and gas pressure was measured with an Omega pressure meter (Omega Engineering). The concentration of O_2 in liquid [O_2(aq)] in the stirred cultures was determined from a saturation of 236 μM O_2 in freshwater with air at 760 mmHg and a temperature of 30°C. The amount of O_2 in the incubation tubes was determined after corrections for changes in pressure and verified based on changes in the N_2:O_2 ratio. After injection of 1.67% O_2(g) in the gas phase, the O_2(g) concentration decreased to ~1.4–1.5% [~16.7 μM O_2(aq)] ~24 h after the nutrients had been autoclaved, due to chemical oxidation of secondary sulfides ($S_2O_3^{2?}+S^0 = H_2S_x$; $2S_xH^? + ½\ O_2 = S^0 + H_2O$). For rapid initiation of the exponential growth phase (~24 h), 6–10 ml medium were inoculated with ~10^6–10^7 cells from liquid cultures of exponentially growing *M. magneticum* strain AMB-1 and incubated at 30°C.

Monitorition of cell growth. Cell growth was monitored as the change in A_{420} (using a HP 8452 diode array spectrophotometer); cell density (in cells/ml) was estimated from a calibration of A_{420} against direct cell counts as determined by optical microscopy. Total protein content was determined by the Lowry method [22], and total iron content by the phenantroline method with hydroxylamine reduction [15] after acid extraction of the cell pellets with 5 M HCl. The magnitude of the magnetic field (B_o) was measured with a triaxial fluxgate magnetometer with a Hall probe (FGM-5DTAA, Walker Scientific) in the 10^{-8}–10^{-5} T range, and with a gaussmeter (Walker Scientific) in the 10^{-5}–10^{-3} T range. MMP expression was monitored according to the relative magnetite load (RML), which was derived from changes in light scattering, according to B_o of ~4×10^{-3} T, along the light path during spectrophotometric measurements.

$$RML = (B–A)/A \quad (1)$$

where: $A = A_{420}$ without applied B_o and $B = A_{420}$ with applied B_o.

In our opinion, RML is a better quantifier of MMP expression than the direct difference B–A (Eq. 1) [38], because RML includes a correction for cell density. The two methods were compared in the analysis of cumulative data from 4 days of readings of 21 tubes. The results showed that in the 17–80 μM O_2(aq) range there was better correlation between [O_2(aq)] and RML ($R^2 = 0.7074$, n = 54) than between [O_2(aq)] and (B–A) ($R^2 = 0.093$, n = 54).

Transmission electron microscopy (TEM). Cells were fixed in 2.5% glutaraldehyde, post-fixed in 1% OsO_4, and stained with saturated uranyl acetate in 70% EtOH. Samples were subsequently dehydrated in an EtOH series and embedded in LR-White resin (London Resin, England). A Sorval Porter-Blum MT2-B ultramicrotome was used to cut ~75-nm thin sections, which were mounted on carbon-coated copper grids. TEM images were obtained on an Akashi EM-002B microscope at 100 keV.

Magnetic and XRD measurements. Exponentially growing cells were harvested by centrifugation under 100% N_2. Magnetic measurements included $FC_{(2.5T)}/ZFC_{(2.5T)}$ remanent magnetization curves, hysteresis loops, and ZFC/FC induced magnetization curves, and were carried out with a MPMS-XL SQUID magnetometer (Quantum Design). $FC_{(2.5T)}/ZFC_{(2.5T)}$ remanent magnetization curves [40] were obtained by cooling the samples from 300 to 5 K in a 2.5-T field ($FC_{2.5T}$) and then measuring magnetization, as the temperature was increased stepwise, in a zero field. Then, the samples were again cooled from 300 to 5 K, but in a zero field, subjected to low-temperature isothermal remanence in a 2.5-T field ($ZFC_{2.5T}$), and magnetization was measured during warming of the samples in a zero field. The $FC_{(2.5T)}/ZFC_{(2.5T)}$ remanence curves allowed whole cells, MMP, and synthetic

magnetite to be distinguished based on the parameter δ, which is a measure of the remanence lost by warming magnetite particles through the Verwey transition (T_V) at 120 K [26,27].

$$\delta = [M_{irm}(80) - M_{irm}(150)]/M_{irm}(80) \quad (2)$$

where M_{irm} is the initial saturation of isothermal remanent magnetization (SIRM) remaining at 80 and 150K for $FC_{(2.5T)}$ and $ZFC_{(2.5T)}$ curves [26].

The δ_{FC}/δ_{ZFC} ratio is diagnostic of magnetite magnetosomes. For intact chains of unoxidized magnetite magnetosomes, the δ_{FC}/δ_{ZFC} ratio is >2 [26]; for maghemite samples, the δ_{FC}/δ_{ZFC} ratio is close to one, but in this case δz_{FC} and δ_{FC} have values of about 0.05–0.06, while the δ_{FC} values for magnetite magnetosomes are larger (~0.08–0.3). Hysteresis loops, or measurements of magnetization (M) as a function of applied field (H), were obtained by applying fields up to 5 T at 300 K. To investigate the presence of superparamagnetic (SPM) behavior, ZFC/FC induced magnetization curves were obtained as follows: the samples were cooled in a zero field from a high temperature (in which all particles show SPM behavior) to a low temperature after which magnetization was measured, as the temperature was increased stepwise from 2 to 300 K (ZFC process), in a small applied field (B_o = 5 mT). The sample was again cooled in the same small field and FC magnetization curves were obtained by measuring magnetization of the samples in the field during a stepwise increase in temperature. Several distinct features of superparamagnetism can be verified from these ZFC/FC measurements, such as the blocking temperature (T_B) peak of the ZFC magnetization curve. Mössbauer spectra were acquired at room temperature and a conventional constant-acceleration spectrometer (Wissel) was used in transmission geometry with a ^{57}Co/Rh source, using α-Fe at room temperature to calibrate isomer shifts and velocity scale. Fitting was obtained by considering a distribution of quadrupole splitting values.

Results

In many applications involving MB, it is impractical to monitor and correct the O_2(g) concentration daily. It would therefore be very useful to determine specific initial culture and incubation conditions that result in cells with a high abundance of arrested growth magnetosomes after a specific time interval or growth stage, without the need for further manipulation. One approach to this problem is to determine the different initial concentrations of O_2(g) and to stir the cultures to avoid the formation of redox gradients in the liquid column. Accordingly, we verified growth and changes in RML at different initial O_2(g) in stirred (150 rpm) vs. unstirred (27 ml Hungate tubes with 10 ml liquid at ~1 bar) cultures. In the 0–147 μM initial O_2(aq) range, stirring the cultures at high O_2 resulted in faster exponential growth of the cells and larger cell densities in the stationary phase (up to ~5×10^8 cells/ml, ~0.28 g dry weight/l after 72 h). Growth was inhibited above 13.2 % initial O_2(g) (>147 μM O_2(aq) in the stirred cultures), while magnetite formation was strongly inhibited in all stirred tubes with >3.9% initial O_2 (Fig. 1). This inhibition was attributed to oxidative stress because magnetite growth requires a ~2:1 Fe(III):Fe(II) ratio, while chemical iron oxidation is fast and has a high equilibrium constant at neutral pH [17,25]. TEM analysis of the non-stirred cultures showed a dominance of large magnetosomes irrespective of the initial O_2 concentration, a lower number of MMP per cell at the highest initial O_2(g), and no sizable increase in the abundance of dwarf MMP. In stirred cultures, however, cells incubated in 0.8% initial O_2(g) [~8.9 μM O_2(aq)] formed mostly normal MMP. A high abundance of dwarf MMP and very few mature MMP was obtained at 5.4% initial O_2(g) [~60.3 μM O_2(aq)],

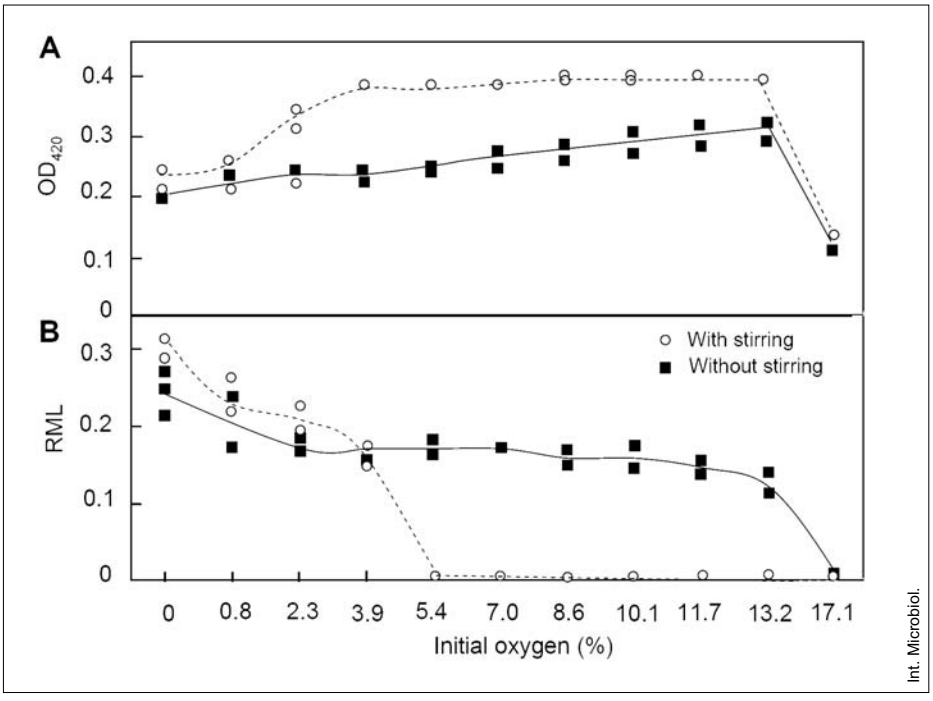

Fig. 1. The effect O_2 on growth (**A**) and relative magnetite load (RML) (**B**) in liquid cultures of *Magnetospirillum magneticum* strain AMB-1 with/without stirring (150 rpm). The initial O_2 values are concentrations in the gas phase at 1 bar.

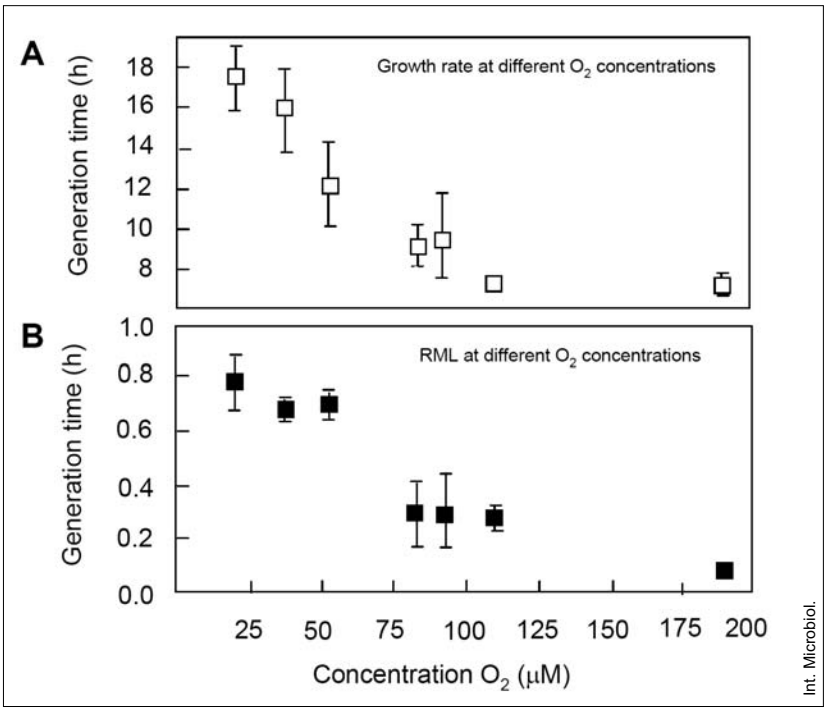

Fig. 2. (**A**) The growth rate of *Magnetospirillum magneticum* strain AMB-1, measured during exponential growth at 24-h intervals, increases with [O_2(aq)], reaching a maximum at 110 μM O_2(aq). (**B**) MMP expression was inhibited at higher [O_2], dropping sharply between 53 and 74 μM O_2(aq). The O_2 concentrations indicated in the graph are averages between triplicate tubes measured after 24 and 48 h of incubation and after corrections were made for changes in pressure. During this 24-h interval the O_2 concentration did not decrease by >20%. Error bars are 1 SD.

and very few, mostly dwarf, MMP were formed by cells incubated at 10.1% initial O_2(g) [~112 μM O_2(aq)]. These results suggested a simple, practical means to obtain arrested growth in MMP without daily monitoring and manipulation of the gas composition, by adjusting the initial gas composition to the correct [O_2] values and by stirring the cultures.

During incubation, the O_2 concentration decreases due to chemical oxidation and respiration, which makes it difficult to identify O_2 conditions optimal for the expression of dwarf MMP. It was therefore necessary to limit depletion of the O_2 pool and to monitor its evolution. This was accomplished using stirred cultures with a larger gas:liquid ratio (27 ml Hungate tubes with 7 ml of liquid culture) and by increasing the initial gas pressure to 1.2–1.4 bar. Under these conditions the O_2(g):O_2(aq) molar ratio was ~125:1 at 30°C and pH 7. Gas pressure, cell density, RML, O_2(g), and N_2(g) were monitored daily in 21 culture tubes containing AMB-1 at seven initial O_2(g) concentrations in the range 17–225 μM O_2(aq). Controls consisted of 21 tubes treated the same way but without cells. Exponential growth occurred between 24 and 48 h in all tubes containing cells. During this 24-h interval, the O_2 concentration did not decrease by more than 25% and the generation time was shorter at higher O_2 concentrations (Fig. 2). The average O_2(g) values between the 24- and 48-h readings for the seven O_2 treatments were 20, 37, 53, 74, 92, 110, and 190 μM. The negative correlation between growth rate and magnetite production in the 20–92 μM O_2(aq) range (Fig. 2B) indicated that that the O_2 conditions optimal for the growth of strain AMB-1 are independent of those optimal for MMP development. The sharpest drop in RML occurred in the 53–74 μM O_2(aq) range.

After 96 h of incubation, O_2 consumption due to respiration was about four times larger than the effect of chemical oxidation (Fig. 3A). Yet, because respiration is sensitive to changes in [O_2], it is generally recommended to avoid interpreting respiration results when [O_2] changes by ≥ 30% between successive readings. For this reason, and because cells in the lag and stationary phases may express different respiration values, O_2 respiration was calculated only during the 24-h interval that corresponded to exponential growth (24–48 h). To calculate the total O_2 respired by cells of strain AMB-1, corrections were made for changes in pressure and for chemical oxidation, predicted from controls at similar [O_2(aq)]. A positive correlation (R^2 = 0.7609; n = 20) was found between the respiration rate and [O_2(aq)], such that μmol O_2 respired × 10^{-10}cells/h = 1.00608 + 0.03299 × [O_2(aq)] (in μM). A comparison of the changes in RML during growth at different initial O_2 concentrations showed that cells of strain AMB-1 formed magnetosomes mostly during exponential growth (Fig. 3B) and that a subsequent drop to <100 μM O_2(aq) at 72 and 96 h, after cells entered the stationary phase, did not restore the RML (results not shown). The expression of MMP remained low in all cultures in which the initial [O_2(aq)] was >100 μM. It must be emphasized here that these results are dependent on culture stirring; without stirring, cells form large amounts of MMP even at high [O_2(g)].

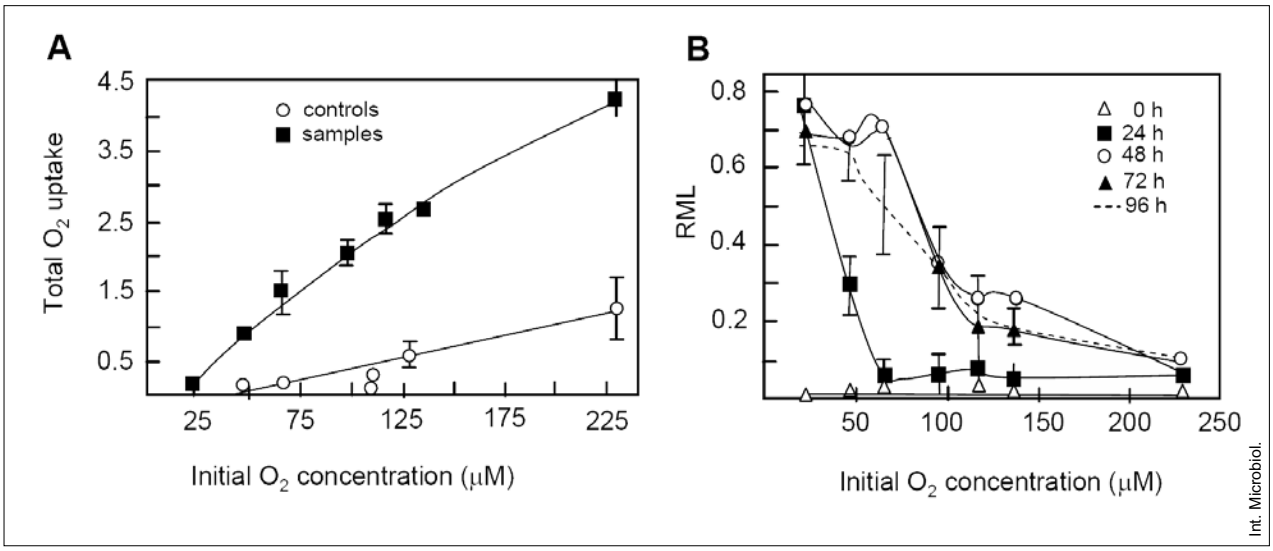

Fig. 3. (**A**) Overall O_2 consumption during the incubation of strain AMB-1 cultures, measured after 96 h. The relative contributions of chemical oxidation (controls) and chemical oxidation plus O_2-respiration (samples) are shown. (**B**) Changes in MMP expression (measured as RML) during incubation with different initial [O_2(aq)] indicate that maximum MMP expression is reached at the end of the exponential phase (48 h in this culture).

Magnetic bacteria also store iron in inorganic deposits other than magnetosomes, such as ferritin granules [5] and vacuoles enriched in amorphous iron phosphate [9]. Although such iron reserves are difficult to quantify, they may play important roles in the ability of the cells to form magnetosomes. In addition, the dynamics of these non-MMP deposits may be controlled by oxidative stress and are thus connected with the growth of MMP. Accordingly, total iron content of *M. magneticum* strain AMB-1 cells was measured in four treatments (18.6 vs. 50 μM O_2(aq), and 0 vs. 150 rpm). To limit changes in [O_2] during incubation, filter-sterilized gas mixtures (O_2 in N_2) containing 1.7 and 4.5% O_2, respectively, were injected every 12 h; the pressure was kept at ~1.3–1.4 bar. Cells were sampled after 48 h (upper exponential phase). The iron content was: 3.8 ± 0.1 mg Fe/mg protein in the 18.6 M O_2(aq)/0 rpm treatment, 2.5 ± 0.2 mg Fe/mg proteins in the 18.6 M O_2(aq)/150 rpm treatment, 5.6±0.5 mg Fe/mg proteins in the 50 mM O_2(aq)/0 rpm treatment, and 1.7 ± 0.2 mg Fe/mg proteins in the 50 μM O_2(aq)/150 rpm treatment. Surprisingly, although RML was larger in the 18.6 μM O_2(aq) treatments, the 50 μM O_2(aq)/0 rpm cultures accumulated the largest amount of iron. Except for the 50 μM O_2(aq)/150 rpm treatment (which resulted mostly in dwarf MMP), all other treatments led to ~95–100% normal MMP. Since dwarf MMP are only 15% of the size of mature MMP (Fig. 4), a significant part of the iron from cells grown at 50 μM O_2(aq) is probably not stored in magnetosomes. However, given the variability of these measurements, the obstacles to exactly measuring the average number of MMP per cell, and the as-yet unclear relationship between RML and the amount of magnetite made, it was difficult to quantify the intracellular non-MMP iron deposits.

The ultrastructure and arrangement of MMP resulting from the different treatments were analyzed by TEM (Fig. 4). The cells were incubated for 4 days at 30°C in 140-ml serum bottles with 50 ml of liquid medium. In the O_2-stress treatments, premixed gas was injected daily to maintain a concentration of 4% in the gas phase (~45 μM). Under 0% O_2 (0 rpm, or 150 rpm) and 4% initial O_2 (at 0 rpm), only normal mature MMP were formed, with no notable differences between treatments. The mature MMP were euhedral, 59 ± 5 nm vs. 42 ± 7 nm in size within the single domain of magnetite. In contrast, MMP formed under O_2 stress (45 μM O_2; 150 rpm), were smaller, non-euhedral spheroids, ~25 ± 4 nm (hence dwarf MMP), with some as small as 10 nm. If dwarf MMP are made solely of magnetite (see below), this size is still within the single domain. A few of these particles (generally <10%) had elongated shapes (1.5:1 length:width ratio) but still were not euhedral. Dwarf MMP were also present in cells with normal MMP, albeit at low abundance (~12–14%). In cells with dwarf MMP, a slightly elevated number (11 ± 2% vs. ~5 ± 2% in cells with normal MMP) of non-aligned MMP were found. The total number of MMP per cell was almost the same between treatments, ranging between 8 and 25 per cell; however, the total number of MMP per cell observed by TEM thin sections has to be taken as an underestimate. Dwarf MMP (≤25 nm) were also found in cells with normal MMP, but they represented ≤5% of the population and were more frequently distributed toward the ends of the chain, suggesting terminal growth of the MMP chain. In cells placed

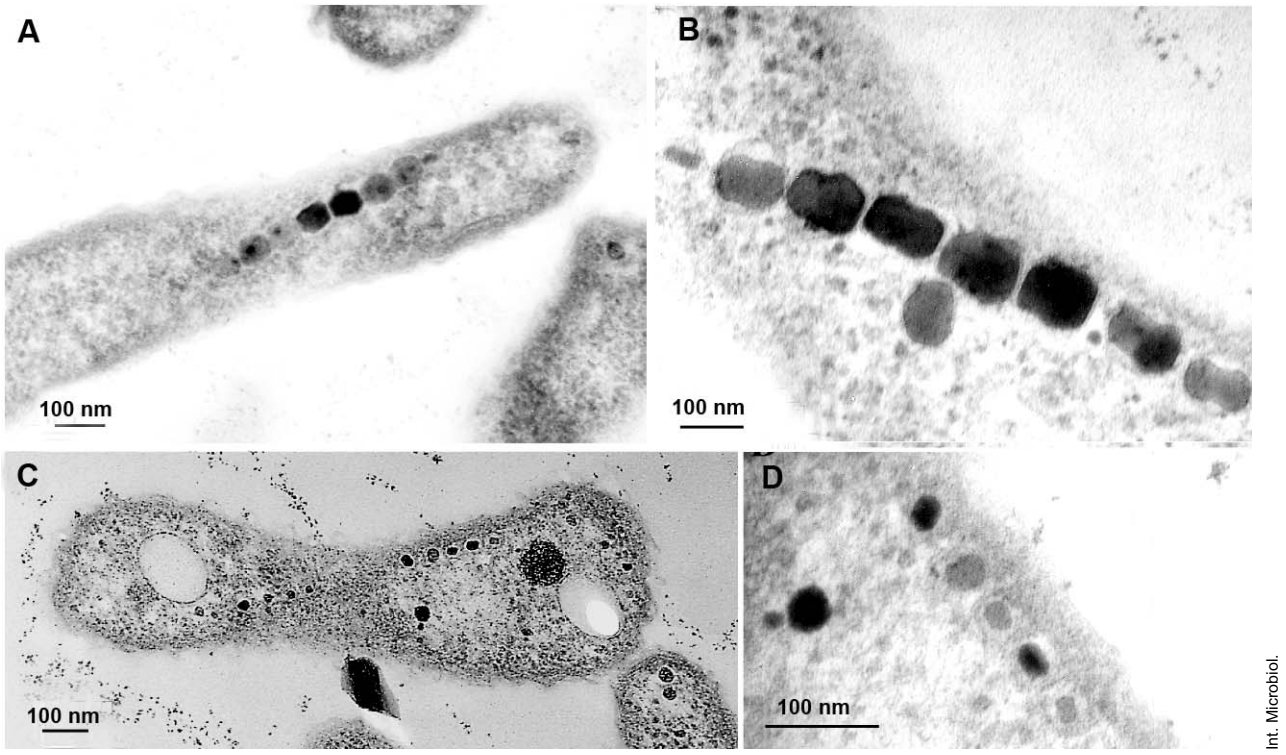

Fig. 4. Transmission electron micrographs of magnetosomes from cells of *Magnetospirillum magneticum* strain AMB-1. (**A**) Normal MMP formed under 0% N_2 and 150 rpm. (**B**) Normal MMP observed at ca. 140,000× magnification. (**C**) Dwarf MMP formed under 4% O_2 and 150 rpm. (**D**) Dwarf magnetosomes observed at ca. 140,000× magnification.

under O_2 stress (45 μM O_2; 150 rpm), the abundance of dwarf MMP was very high (>95%). Without exception, no more than one MMP was ever found per magnetosome vesicle, although a few vesicles (~3–4%) did not contain MMP. In some TEM images, positive identification of some of the vesicles and of the dwarf MMP was difficult. There was no significant difference in the abundance of empty MMP vesicles between the different treatments, indicating that 45 μM O_2(aq) stress did not inhibit nucleation but only MMP growth. The morphology of the few dwarf MMP contained in cells with normal MMP was very similar with the morphology of the dwarf MMP from cells subjected to O_2 stress. Euhedral MMP <20 nm in size were never found, irrespective of the treatment.

To address whether dwarf MMP are similar in composition to normal MMP, cells with normal and dwarf MMP were compared during two different treatments: ~18.7 μM O_2/150 rpm (for normal MMP) and O_2-streesed cultures ~45 μM O_2/150 rpm (for dwarf MMP). The large amounts of samples needed for the magnetic measurements were obtained by culturing the cells in 1- to 2-l serum bottles with 20–25% liquid medium (as shown in Materials and methods). The medium was autoclaved with ~1.67% O_2 in the gas phase and the gas composition adjusted after cooling to the desired [O_2], adjusted the pressure at ~1 bar. One ml of inoculum from a culture of AMB-1 in late exponential phase was added per liter and the cultures incubated for 72 h at 30°C. After centrifugation, the pellet obtained from cultures with normal MMP was dark-gray to black, uniform, with a thin white upper layer, while pellets of cells with dwarf MMP were heterogeneous. The upper part of the pellet (~90%) was white, while the bottom part was gray with black spots. We assumed that this heterogeneity was due to cells with different abundances of dwarf MMP, or to a small population of normal size magnetosomes still present in the O_2-stressed cultures, or to an agglomeration of MMP as a result of centrifugation and poor chain alignment. TEM analysis of these pellets indicated that dwarf MMP were present, abundant, and similar in both the upper and lower parts of the pellets of O_2-stressed cells, and that the sizes of the MMP did not significantly differ between these subsamples.

We then sought to determine whether different parts of the O_2-stressed cell pellets contained the same type of magnetic materials. Three types of samples were compared: (A) pellets of cells with normal MMP, (B) the upper, white part of the pellets with dwarf MMP, and (C) the lower, dark part

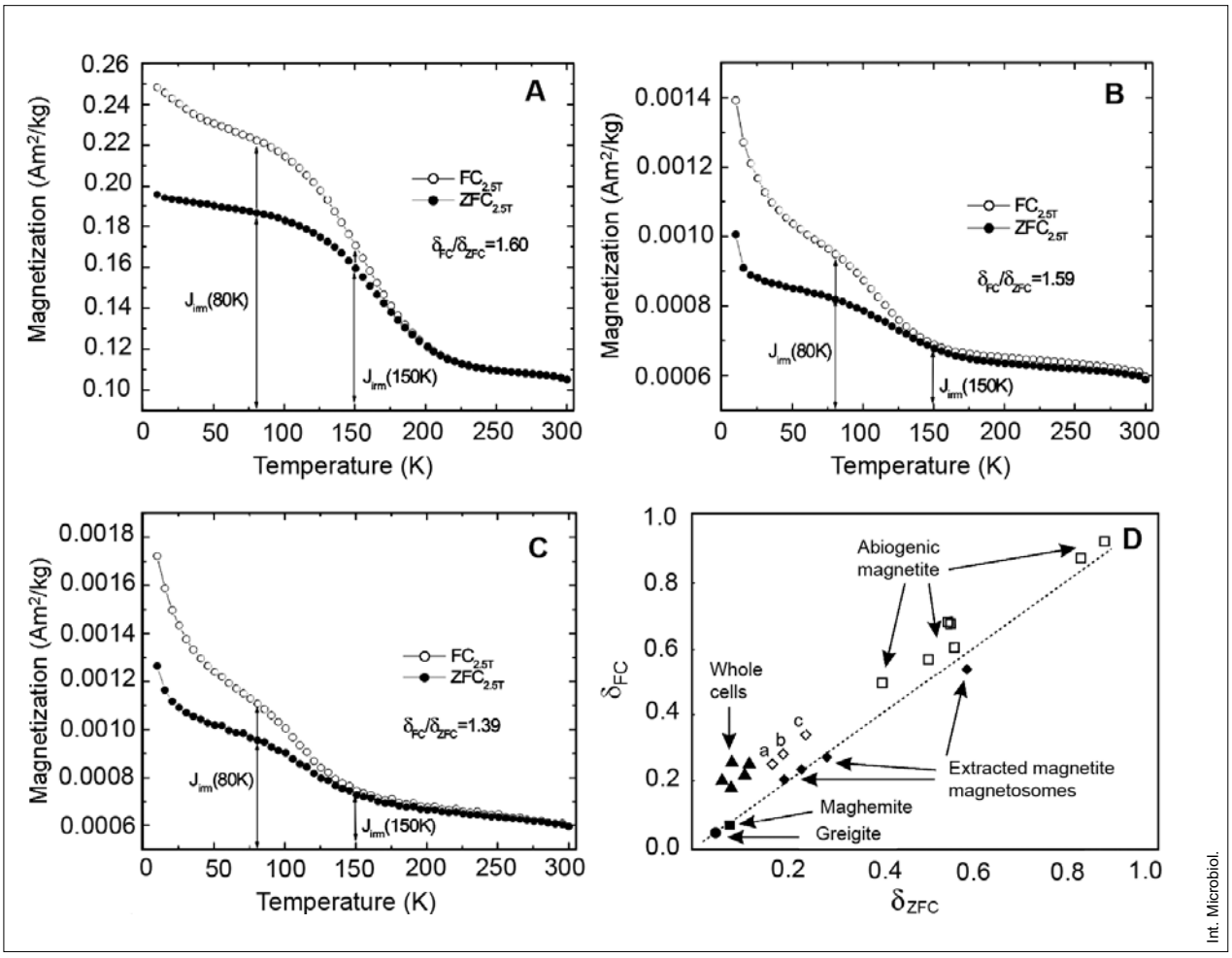

Fig. 5. $FC_{(2.5T)}/ZFC_{(2.5T)}$ remanent magnetization curves showing Verwey transitions and δ_{FC}/δ_{ZFC} ratios. (**A**) Pellet of cells with normal MMP. (**B**) Upper part of the cell pellet containing dwarf MMP. (**C**) Lower part of the cell pellet containing dwarf MMP. (**D**) δ_{FC}/δ_{ZFC} plot of the A, B, and C samples relative to data on other published samples [26].

of the pellets with dwarf MMP. The $FC_{(2.5T)}/ZFC_{(2.5T)}$ remanent magnetization curves showed very similar patterns between samples B and C, and all samples had Verwey transitions at ~120 K, characteristic for magnetite (Fig. 5). The contribution of paramagnetic (PM) materials was larger in B and C than in normal MMP samples; this was partly expected because cells with dwarf MMP have less Fe and magnetite than cells with normal MMP. All samples showed a δ_{FC}/δ_{ZFC} behavior between whole cells and extracted magnetosomes; which was also expected since dwarf MMP were not extracted from the cells, in order to limit dissolution, oxidation, and chain breakage. A value of ~1 for δ_{FC}/δ_{ZFC} indicates isolated magnetite particles while a value of ~2 indicates perfectly aligned magnetite chains [26]. No significant differences in the level of alignment between B (δ_{FC}/δ_{ZFC} = 1.59) and A (δ_{FC}/δ_{ZFC} = 1.60) were found whereas smaller values (δ_{FC}/δ_{ZFC} = 1.39), an indication of poorer alignment, were obtained for C. It was previously observed [26] that the conversion of magnetite MMP to maghemite (such as during oxidation) reduces δ_{FC} and δ_{ZFC} close to 0.05–0.06 and brings the δ_{FC}/δ_{ZFC} ratio to ~1. We found δ_{FC}/δ_{ZFC} ratios <2 and thus inferred no evidence of magnetite alteration.

Samples A, B, and C (Fig. 5) were also compared by hysteresis loop analysis (data not shown). Paramagnetic (PM) and ferrimagnetic contributions in all samples were recorded. In addition, the PM effect was stronger in samples with dwarf MMP, supporting the results presented above (namely, Fe composition and $FC_{(2.5T)}/ZFC_{(2.5T)}$ ratio). The hysteresis parameters at 300 K, the saturation magnetization (M_s), and the saturation remanent magnetization (M_{rs}) were very similar between the A and B samples. Using the known value of M_s for magnetite, we estimated that the dried-pellet samples each contained <1% magnetite. Additional information was obtained from the M_{rs}/M_s ratio, which for whole-cell samples

at room temperature is ~0.5 for a random distribution of uniaxial "single domain chains" [26]. The values obtained for the A and B samples were smaller than expected (~0.4); this may have been due to broken chains, which is a typical artifact of extended centrifugation. It was difficult to determine a precise M_{rs}/M_s value for the C samples because of their high PM contribution. Mössbauer spectra showed only doublets, which may have indicated PM or SPM iron phases, thus confirming previous reports [12], but ZFC/FC induced magnetization analysis showed only PM and not SPM behavior. Lastly, XRD analysis showed no significant differences between samples and that the only mineral present was magnetite (results not shown), supporting the previous results.

Discussion

It was previously reported that the expression of MMP in *M. magneticum* strain AMB-1 is optimal at 2.35 μM O_2, is partly inhibited at 11.7 μM O_2, and totally inhibited at 23.52 μM O_2. Without subsequent manipulation of the gas composition, we found that *M. magneticum* strain AMB-1 cells are more tolerant to O_2 stress than previously acknowledged, when an inorganic reductant (such as $S_2O_3^{2-}$:S^0 mixture) is added to the medium. During these incubations, O_2 decreased by 6–45% over 96 h. The initial culture conditions described herein allow a high abundance of dwarf MMP to be obtained without the need for chemical monitoring and periodic adjustment of [O_2]. Cells of *M. magneticum* strain AMB-1 grew better at 100–225 μM O_2(aq) in stirred liquid culture than at lower [O_2], yet the formation of MMP was repressed at ~45 μM O_2(aq) and strongly inhibited at ≥100 μm O_2(aq). Under conditions of ~45 μM initial O_2 in liquid, 150 rpm, and 30°C, numerous dwarf magnetosomes, representing ≥ 95% of the total MMP population, formed after 48 h of incubation, and the O_2 concentration decreased by ~20%. The higher respiration rate, faster growth, and higher final density at higher [O_2] supports the conclusion that, in strain AMB-1, the oxidative stress of MMP production does not coincide with the oxidative discomfort of the cells.

The total number of MMP was similar between cells with normal MMP and cells with dwarf MMP grown at 45 μM initial O_2(aq) and 150 rpm. Only a small fraction of all dwarf MMP were not aligned. Magnetite was the only magnetic material or mineral detected in strain AMB-1. The smallest dwarf magnetosomes were ~10 nm in size and were very seldom euhedral, but rather irregular spheroids. MMP vesicles with more than one MMP particle were not observed, implying that MMP are initiated from a sole nanocrystallite and novel magnetosome were added mainly terminally in the MMP chain. Despite the fact that very large populations of dwarf MMP were analyzed (~4×10^{11} per sample), there were no signals of SPM behavior; instead, only SD behavior and PM signal. The magnetic signatures of cells with dwarf MMP was nearly the same as that of cells with normal magnetosomes, i.e., no ferryhydrite, aligned SD magnetite, no SPM behavior, and enrichment in PM iron.

In earlier models, it was hypothesized that MMP are initiated via: (i) SPM nanocrystallites of magnetite growing into mature single domain particles; (ii) early granules of crystalline or amorphous ferryhydrite, later replaced by magnetite [11,37]; or (iii) iron-rich organic matrices, later replaced by magnetite [23,45]. The existence of a short-lived SPM magnetite or ferryhydrite phase during MMP growth cannot be excluded, but a method to systematically stop the growth of all magnetosomes in very early SPM stages has yet to be found. The MMP were not in physical contact with the MMP membrane, perhaps indicating that the growth of MMP is controlled via solute chemistry rather than surface contact. The initiation of novel MMP was not observed, probably because the period of growth between early nanocrystallites and dwarf MMP is very short. The culturing conditions proposed herein have a greater effect on the growth of MMP from dwarf to mature MMP than on the formation of dwarf MMP, and can be used to study stages in MMP development.

Acknowledgements. This research was supported by grants from NASA (Astrobiology Institute, Planetary Biology Internship), National Science Foundation (NSF), and the University of Southern California Undergraduate Research Program. Special thanks to Dr. S. Lund of the USC for help with calibrating RML readings vs. the abundance of cellular magnetite. This study was also supported by NSF grant EAR 0311869, from the Biogeosciences program, the Institute for Rock Magnetism (IRM), funded by the Earth Science Division of NSF, and the W. M. Keck Foundation and University of Minnesota, IRM publication # 0613.

References

1. Abreu F, Silva KT, Martins JL, Lins U (2006) Cell viability in magnetotactic multicellular prokarayotes. Int Microbiol 9:267-272
2. Abreu F, Silva KT, Farina M, Keim CN, Lins U (2008) Greigite magenetosome membrane ultrastructure in '*Candidatus* Magnetoglobus multicellularis'. Int Microbiol 11:75-80
3. Bazylinski DA, Frankel RB (2003) Biologically controlled mineralization in prokaryotes. In: Dove PM, De Yoreo JJ, Weiner S (eds) Biomineralization, Reviews in Mineralogy and Geochemistry, Vol. 54. Min Soc Amer Geochem Soc, pp 217-247
4. Bazylinski DA, Moskowitz BM (1997) Microbial biomineralization of magnetic iron minerals: Microbiology, magnetism and environmental significance. Rev Mineral 35:181-223
5. Bertani LE, Huang JS, Weir BA, Kirschvink JL (1997) Evidence for two types of subunits in the bacterioferritin of *Magnetospirillum magnetotacticum*. Gene 201:31-36
6. Blakemore RP (1975) Magnetotactic bacteria. Science 190:377-379

7. Blakemore RP (1982) Magnetotactic bacteria. Annu Rev Microbiol 36:217-38
8. Blakemore RP, Short RA, Bazylinski C, Rosenblatt C, Frankel RB (1985) Microaerobic conditions are required for magnetite formation within *Aquaspirillum magnetotacticum*. Geomicrobiol J 4:53-71
9. Cox BL, Popa R, Bazylinski DA, Lanoil B, Douglas S, Belz A, Engler DL, Nealson KH (2002) Organization and elemental analysis of P-, S-, and Fe-rich inclusions in a population of freshwater magnetococci, Geomicrobiol J 19:387-406
10. Frankel RB (1981) Bacterial magnetotaxis vs. geotaxis. Trans Am Geophys Soc (EOS) 62:850
11. Frankel RB, Papaefthymiou GG, Blakemore RP, O'Brien W (1983) Fe_3O_4 precipitation in magnetotactic bacteria. Biochim Biophys Acta 763:147-159
12. Frankel RB, Papaefthymiou GC, Blakemore RP (1985) Mössbauer spectroscopy of iron biomineralization products in magnetotactic bacteria. In: Kirschvink JL, Jones DS, MacFadden BJ (eds) Magnetite biomineralization and magnetoreception in organisms. Plenum, New York, pp 269-287
13. Frankel RB, Bazylinski DA, Johnson MS, Taylor BL (1997) Magneto-aerotaxis in marine coccoid bacteria. Biophys J 73:994-1000
14. Gorby YA, Beveridge TJ, Blakemore RP (1988) Characterization of the bacterial magnetosome membrane. J Bacteriol 170:834-841
15. Greenberg AE, Trussell RR, Clesceri LS (eds) (1985) Standard methods for the examination of water and wastewater, 16th ed. APHA-AWWA-WPCF, Port City Press, Baltimore
16. Grunberg K, Wawer C, Tebo BM, Schuler D (2001) A large gene cluster encoding several magnetosome proteins is conserved in different species of magnetotactic bacteria. Appl Environ Microbiol 67:4573-4582
17. Heyen U, Schüler D (2003) Growth and magnetosome formation by microaerophilic *Magnetospirillum* strains in an oxygen-controlled fermentor. Appl Microbiol Biotechnol 61:536-544
18. Kawaguchi R, Burgess JG, Sakaguchi T, Takeyama H, Thornhill RH, Matsunaga T (1995) Phylogentic analysis of a novel sulfate-reducing magnetic bacterium, RS-1, demonstrates its membership of the Proteobacteria. FEMS Microbiol Lett 126:277-282
19. Keim CN, Solórzano G, Farina M, Lins U (2005) Intracellular inclusions of uncultured magnetotactic bacteria. Int Microbiol 8:111-117
20. Kirschvink JL (1982) Birds, bees and magnetism: A new look at the old problem of magnetoreception. Trends Neuroscien 5:160-167
21. Komeili A, Vali H, Beveridge TJ, Newman DK (2004) Magnetosome vesicles are present before magnetite formation, and MamA is required for their activation. Proc Natl Acad Sci USA 101:3839-3844
22. Lowry OH, Rosebrough NJ, Farr AL and Randall RJ (1951) Protein measurement with the Folin-Phenol reagents. J Biol Chem 193:265-275
23. Matsunaga T, Okamura Y (2003) Genes and proteins involved in bacterial magnetic particle formation. Trends Microbiol 11:536-541
24. Matsunaga T, Okamura Y, Tanaka T (2004) Biotechnological application of nano-scale engineered bacterial magnetic particles. J Mater Chem 14:2099-2105
25. Matsunaga T, Sakaguchi T, Tadokoro F (1991) Magnetite formation by a magnetic bacterium capable of growing aerobically. Appl Microbiol Biotechnol 35:651-655
26. Moskowitz BM, Frankel RB, Bazylinski DA (1993) Rock magnetic criteria for the detection of biogenic magnetite. Earth Planet Sci Lett 120:283-300
27. Moskowitz BM, Frankel RB, Flanders PJ, Blakemore RP, Schwartz BB (1988) Magnetic properties of magnetotactic bacteria. J Magn Magn Mat 73:273-288
28. Nakamura CJ, Burgess G, Sode K, Matsunaga T (1995) An iron-regulated gene, *magA*, encoding an iron transport protein of *Magnetospirillum* sp. strain AMB-1. J Biol Chem 270:28392-28396
29. Okamura Y, Takeyama H, Matsunaga T (2001) A magnetosome-specific GTPase from the magnetic bacterium *Magnetospirillum magneticum* AMB-1. J Biol Chem 276:48183-48188
30. Paoletti LC, Blakemore RP (1986) Hydroxamate production by *Aquaspirillum magnetotacticum*. J Bacteriol 167:73-76
31. Sakaguchi T, Tsujimura N, Matsunaga T (1996) A novel method for isolation of magnetic bacteria without magnetic collection using magnetotaxis. J Microbiol Meth 26:139-145
32. Scheffel A, Gruska M, Faivre D, Linaroudis A, Plitzko JM, Schuler D (2006) An acidic protein aligns magnetosomes along a filamentous structure in magnetotactic bacteria. Nature 440:110-114
33. Schüler D (1999) Formation of magnetosomes in magnetotactic bacteria. J Molec Microbiol Biotechnol 1:79-86
34. Schüler D (2002) The biomineralization of magnetosomes in *Magnetospirillum gryephiswaldense.* Int Microbiol 5:209-214
35. Schüler D, Baeuerlein E (1997) Iron transport and magnetite crystal formation of the magnetic bacterium *Magnetospirillum gryphiswaldense*. J Physiq IV 7(C1):647-650
36. Schüler D, Baeuerlein E (1998) Dynamics of iron uptake and Fe_3O_4 biomineralization during aerobic and microaerobic growth of *Magnetospirillum gryphiswaldense.* J Bacteriol 180:159-162
37. Schüler D, Frankel RB (1999) Bacterial magnetosomes: microbiology, biomineralization and biotechnological applications. Appl Microb Biotech 52:464-473
38. Schüler D, Uhl R, Baeuerlein E (1995) A simple light scattering method to assay magnetism in *Magnetospirillum gryphiswaldense*. FEMS Microbiol Lett 132:139-145
39. Short KA, Blakemore RP (1986) Iron respiration-driven proton translocation in aerobic-bacteria. J Bacteriol 167:729-731
40. Smirnov AV, Tarduno JA (2002) Magnetic field control of the low-temperature magnetic properties of stoichiometric and cation-deficient magnetite. Earth Planet Sci Lett 194:359-368
41. Spring S, Amann R, Ludwig W, Schleifer KH, van Gemerden H, Petersen N (1993) Dominating role of an unusual magnetotactic bacterium in the microaerobic zone of a freshwater sediment. Appl Env Microbiol 59:2397-2403
42. Spring S, Schleifer KH (1995) Diversity of magnetotactic bacteria. System Appl Microbiol 18:147-153
43. Steinberger B, Petersen N, Petermann H, Weiss DG (1994) Movement of magnetic bacteria in time-varying magnetic-fields. J Fluid Mech 273:189-211
44. Thomas-Keprta KL, Clemett SJ, Bazylinski DA, et al. (2001) Truncated hexa-octahedral magnetite crystals in ALH84001: Presumptive biosignatures. Proc Natl Acad Sci USA 98:2164-2169
45. Vainshtein MB, Suzina NE, Kudryashova EB, Ariskina EV, Sorokin VV (1998) On the diversity of magnetotactic bacteria. Microbiologiya 67:670-676
46. Walker MM, Kirschvink JL, Chang S-B R, Dizon AE (1984) A candidate magnetic sense organ in the yellowfin tuna *Thunnus albacares*. Science 224:751-753